CREEP OF INITIALLY ANISOTROPIC UNHARDENED MATERIALS

O. V. Sosnin

Utilizing the hypothesis of the existence of a creep-strain-rate potential and assuming it a function of the mixed invariant of the stress tensor and the tensor of the anisotropic characteristics of the material, we show the possibility of an approximate description of the steady creep of a certain class of anisotropic materials, and we carry out an experimental verification of the dependences obtained for the case of creep of tubular samples under tension and torsion.

1. The steady creep of materials under uniaxial loading is usually described by dependences of the form

$$\eta = B\sigma^n, \qquad \eta = Ke^{\beta\sigma} \tag{1.1}$$

Here η is the creep strain rate, σ is the stress, B and n or K and β, respectively, are the experimental characteristics of the material. Anisotropy in the behavior of a material in a description of creep can be manifest both in a change of one of the characteristic quantities in (1.1) depending on the orientation of the applied loading vector in the solid and in their simultaneous variation.

Let us examine a simpler case of anisotropy when the characteristic B or K, respectively, changes in (1.1) and the material behaves identically under creep tension and compression. The creep of such materials can be described by introducing a strain-rate potential in the form

$$\Phi_1 = \left(\frac{T_1}{S}\right)^m (S)^{1/2(n+1)}, \qquad \eta_{ij} = \frac{\partial \Phi_1}{\partial \sigma_{ij}} \tag{1.2}$$

if the first of the dependences (1.1) is taken as the initial dependence and

$$\Phi_2 = \left(\frac{T_2}{S}\right)^m \exp(\beta_1 S^{1/2}), \qquad \eta_{ij} = \frac{\partial \Phi_2}{\partial \sigma_{ij}}$$

$$S = 3\sigma_{ij}^\circ \sigma_{ij}^\circ, \qquad \sigma_{ij}^\circ = \sigma_{ij} - 1/3\,\delta_{ij}\sigma_{kk} \tag{1.3}$$

$$T_1 = A_{11}(\sigma_{22}-\sigma_{33})^2 + A_{22}(\sigma_{33}-\sigma_{11})^2 + A_{33}(\sigma_{11}-\sigma_{22})^2 + 2A_{12}\sigma_{12}^2 + 2A_{23}\sigma_{23}^2 + 2A_{31}\sigma_{31}^2$$

if the second of the dependences (1.1) is taken as initial dependence.

Here T_2 has an analogous form with other coefficients A_{ij}. Hence, in conformity with the structure of (1.1), the potential functions (1.2) and (1.3) consist of the product of two functions: a homogeneous function of zero power in the stresses $(T/S)^m$ taking into account the anisotropy of the material in terms of the coefficient B or K, and a power-law or exponential function with isotropic characteristic n or β_1. Exponent m can be selected arbitrarily; in particular, it is expedient to take $m = 1/2\,(n+1)$ in (1.2) and m = 1 in (1.3), and the dependences (1.2) and (1.3) finally become

$$\Phi_1 = T_1^{1/2(n+1)}, \qquad \eta_{ij} = \partial\Phi_1 / \partial\sigma_{ij} \tag{1.4}$$

$$\Phi_2 = \exp(\beta_1 S^{1/2})\, T_2 / S, \qquad \eta_{ij} = \partial\Phi_2 / \partial\sigma_{ij} \tag{1.5}$$

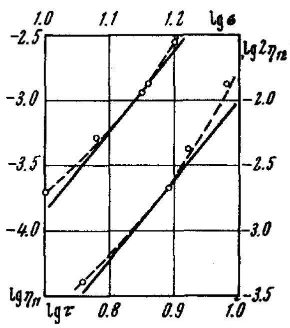

Fig. 1

Figure 1 presents, in a logarithmic coordinate system, results of experiments in the form of a dependence of the magnitude of the steady creep rate in the axial direction $d\varepsilon/dt \equiv \eta_{11}$ on the stresses in tubular samples under pure tension (upper graph) and of the shear rate $d\gamma/dt \equiv 2\eta_{12}$ on the magnitude

Novosibirsk. Translated from Zhurnal Prikladnoi Mekhaniki i Tekhnicheskoi Fiziki, No. 4, pp. 123-127, July-August, 1970. Original article submitted July 17, 1969.

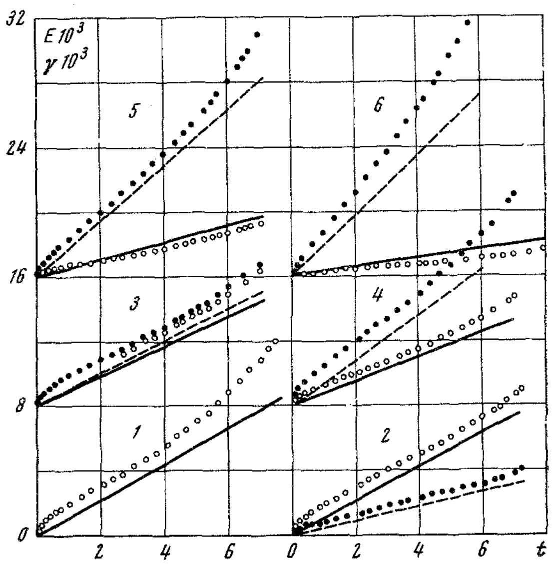

Fig. 2

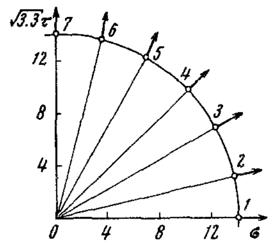

Fig. 3

of the tangential stress τ under pure torsion (lower graph). Tubular samples of 20 and 18 mm outer and inner diameter, respectively, and 80 mm length of the working section were fabricated from a 30-mm-diameter D16T rod and tested at a 250°C temperature. After fabrication, the samples were not heat treated. The heating mode of the samples and its duration were kept constant for 2.5 h from the time of inclusion prior to loading. The stresses were computed from the condition of their uniform distribution over the sample cross section and the equating of the external to the internal torque relative to the mean radius of the cross section.

It is seen from Fig. 1 that it is necessary to utilize a dependence more complex than (1.1) in order to describe the creep process in a broad range of stresses. The characteristics B and n, or K and β, respectively, can be taken as constants only for a narrow band of stresses. Thus, for example, for a stress level on the order of 14 kg/mm² under pure tension, and on the order of 8 kg/mm² for pure torsion, we find from Fig. 1 in application to the first of the dependences (1.1)

$$n = 6, \quad B_\sigma = 1.3 \cdot 10^{-10}, \quad B_\tau = 8.65 \cdot 10^{-9} \qquad [\mathrm{mm}^{2n}/\mathrm{kg}^n \cdot \mathrm{h}] \tag{1.6}$$

Taking the potential function in the form (1.4) and taking account of the axial symmetry of the material, the coefficients in the quadratic form T_1, which is an application to the description of creep under tension and torsion

$$T_1 = (A_{22} + A_{33})\sigma^2 + 2A_{12}\tau^2$$

are determined in terms of the quantities (1.6) [1]:

$$A_{22} + A_{33} = [B_\sigma / (n+1)]^{2/(n+1)} = 0.86 \cdot 10^{-3}, \qquad 2A_{12} = [B_\tau / (n+1)]^{2/(n+1)} = 2.85 \cdot 10^{-3} \tag{1.7}$$

Figure 2 presents results of experiments on the creep of tubular samples of this material under combined tension and torsion, conducted at the same temperature according to the 1 kg/mm² loading program mentioned in Table 1. The open circles on the graphs denote the axial strain ε, and the dark circles denote the shear strain γ, while the time is indicated in hours. The number of the experiment corresponding to Table 1 is noted in the squares. The solid and dashed lines here indicate the computed values, respectively, of the same strains obtained by means of (1.4) with the coefficients (1.7). It is seen from the graphs and Table 1 that, on the whole, the values of the computed creep strain rates η_{ij} in the steady-state stage are similar to the experimental values of the rates η_{ij}^*.

Because of (1.4), the creep-strain-rate vector at any point of the stress state in the $\sigma\,\tau$ plane should be orthogonal to the surface $\Phi_1 = \mathrm{const}$ passing through this stress point.

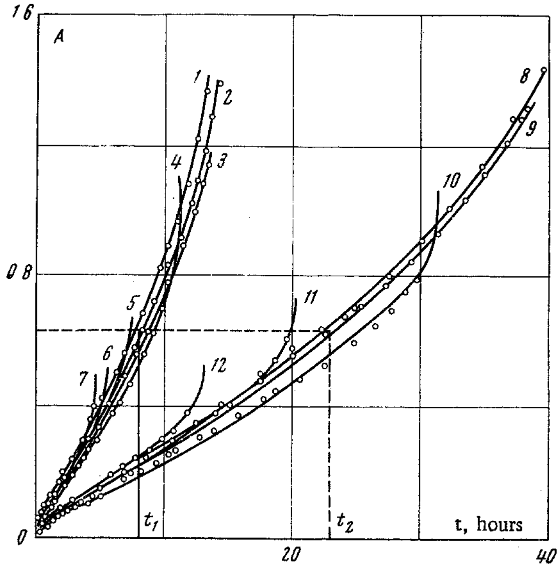

Fig. 4

TABLE 1

	σ	τ	$\overset{*}{\eta}_{11}\cdot 10^3$	$\eta_{11}\cdot 10^3$	$2\overset{*}{\eta}_{12}\cdot 10^3$	$2\eta_{12}\cdot 10^3$	$W_{11}\cdot 10^3$
1	14.18	—	1.15	1.11	—	—	16.3
2	13.80	1.82	1.05	1.03	0.50	0.46	15.4
3	12.35	3.85	0.95	0.93	1.00	0.99	15.6
4	10.25	5.40	0.73	0.75	1.40	1.40	15.0
5	7.00	6.80	0.43	0.53	1.70	1.70	14.6
6	3.50	7.56	0.18	0.26	2.40	1.90	18.8
7	—	7.81	—	—	2.10	2.00	16.4

In the coordinate system σ, $[2A_{12}/(A_{22}+A_{33})]^{1/2}\tau$ the equation $\Phi_1 = \text{const}$ will map a circle. Setting aside points with stress components for which the experiment has been conducted – the quantities $[2A_{12}/(A_{22}+A_{33})]^{1/2}\eta_{11}{}^*$ and $2\eta_{12}{}^*$ measured along the horizontal and vertical, respectively, in the experiment – we obtain the resultant strain-rate vector, which should coincide with the radial direction. The stress state in each of the experiments presented in Fig. 2 was selected so that it would satisfy the equation $\Phi_1 = \text{const}$.

Figure 3 presents the shape of this surface, and the points of the stress states at which the experiments shown in Table 1 were conducted are noted. The directions of the resultant creep-strain-rate vectors constructed according to the data of the experiments are indicated here.

Because of the homogeneity of the potential function relative to the stresses, we obtain from (1.4)

$$\sigma_{ij}\eta_{ij} = (n+1)\Phi_1 \tag{1.8}$$

Therefore, in the stress space the surfaces of constant specific dissipation power $\sigma_{ij}\eta_{ij} \equiv W_1 = \text{const}$ are similar to the surfaces $\Phi_1 = \text{const}$. The values of the creep strain rates in 1/h measured in the steady-state creep stage $\eta_{ij}{}^*$ in the experiments, η_{ij} computed by means of (1.4) with the characteristics (1.6) and (1.7), and the quantities W_1 kg/mm$^2\cdot$h calculated by means of the experimental values are indicated in Table 1. Excluding experiment 6, all the values of W_1 do not emerge beyond the strip of experimental scatter with respect to the mean value which is customary for creep.

According to [2], for processes with identical values of W_1 the magnitude of the specific work dissipated during creep

$$A = \int_0^t \sigma_{ij}\eta_{ij}\,dt$$

at any time should remain identical down to fracture. By making appropriate constructions according to the results in Fig. 2, it is easy to see that the $A = A\ (t)$ diagrams will issue in a compact beam in all the creep stages.

These same results were worked out by means of the second of the dependences (1.1) with the potential flow function Φ_2 introduced in the form (1.5). The coefficients in the quadratic form will have other values as compared with the analogous quantities (1.7), and the shape of the surface $\Phi_2 = \text{const}$ will be different, but a direct computation showed that the stresses satisfying the equations $\Phi_1 = \text{const}$ and $\Phi_2 = \text{const}$ and having a common point differ within 1% limits. Analogous results with the same order of deviation are

TABLE 2

	σ	τ	$W_2 \cdot 10^3$		σ	τ	$W_2 \cdot 10^3$
1	8.00	—	64.0	7	—	4.24	67.5
2	7.71	1.12	65.7	8	7.00	—	24.2
3	6.91	2.13	69.7	9	6.05	1.86	24.8
4	5.66	3.00	61.2	10	4.95	2.62	21.9
5	3.98	3.68	71.0	11	3.48	3.22	23.7
6	2.06	4.10	64.0	12	—	3.71	25.9

obtained also for the creep strain rate components and for the stresses satisfying W_1 = const and W_2 = const with one common point.

2. Experiments on tubular samples cut out of a duralumin slab in the rolling direction were carried out by an analogous program [1]. The slab is 20 mm thick, and in contrast to the samples from the preceding section, the outer and inner diameters of these tubes were 16.5 and 15 mm, respectively.

Describing the one-dimensional creep of the material by the first of the dependences (1.1) and assuming the existence of a creep-strain-rate potential function in the form

$$F = T^{(n+1)/2}, \qquad \eta_{ij} = \partial F / \partial \sigma_{ij}$$

$$T = C_{11}(\sigma_{22} - \sigma_{33})^2 + C_{22}(\sigma_{33} - \sigma_{11})^2 + C_{33}(\sigma_{11} - \sigma_{22})^2 + 2C_{12}\sigma_{12}^2 + 2C_{23}\sigma_{23}^2 + 2C_{31}\sigma_{31}^2 \tag{2.1}$$

as applied to the description of results of experiments on an orthotropic material under simultaneous tension and torsion, we obtain

$$\begin{gathered} \eta_{11} = (n+1)\left[(C_{22} + C_{33})\sigma^2 + (2C_{12}\sin^2\varphi + 2C_{13}\cos^2\varphi)\tau^2\right]^{(n-1)/2} \quad (C_{22} + C_{33})\sigma \\ d\gamma / dt = (n+1)\left[(C_{22} + C_{33})\sigma^2 + (2C_{12}\sin^2\varphi + 2C_{13}\cos^2\varphi)\tau^2\right]^{(n-1)/2}(2C_{12}\sin^2\varphi + 2C_{13}\cos^2\varphi)\tau \end{gathered} \tag{2.2}$$

Here $\sigma_{12} = -\tau \sin\varphi$, $\sigma_{13} = \tau\cos\varphi$, the angle φ is measured from the second direction.

It follows from (2.2) that the rates η_{11} and $d\gamma/dt$ at each point of an annular section are distinct. Because the tube ends are stiff and therefore under the conditions of the experiment the axial rates η_{11} should not depend on φ under combined tension and torsion, the expression

$$(2C_{12}\sin^2\varphi + 2C_{13}\cos^2\varphi)\tau^2 \equiv k^2$$

should not depend on φ, while τ and γ themselves depend on φ. The magnitude of the shear γ averaged over the contour is usually measured in experiment, which permits utilization of average values of the quantity τ over the contour and

$$(2C_{12}\sin^2\varphi + 2C_{13}\cos^2\varphi) \equiv 2C$$

From the results of creep experiments on the samples cut out in the longitudinal direction and subjected to tension at a 200°C temperature it is found [1] that

$$n = 8, \qquad C_{22} + C_{33} = 0.87 \cdot 10^{-20/9} \tag{2.3}$$

and from experiments on the pure torsion of tubular samples cut out in the same direction there has been found the average value of the coefficient 2C for a shear stress τ in the quadratic form T as

$$2C = 3.1 \cdot 10^{-20/9} \quad [\mathrm{mm}^{2n}/\mathrm{kg}^n \cdot \mathrm{h}]^{2/(n+1)} \tag{2.4}$$

Experiments on a complex stress state have been conducted on the kg/mm² loading program indicated in Table 2 and in contrast to the experiments of the preceding section were continued far beyond the limits of the second stage of creep.

The stresses indicated in Table 2 have been selected so that they would satisfy the equation F = const, where the first seven experiments were conducted under the condition that the points mapping the stress state lie on a surface F = const passing through the point $\sigma = 8$ kg/mm², $\tau = 0$ while the mapping points in the remaining five experiments lie on a surface passing through the point $\sigma = 7$ kg/mm², $\tau = 0$. The creep-strain-rate vectors, constructed at appropriate points of the stress state, agree sufficiently well with the direction of the normal to the surface at these points. Moreover, in the experiments with constant stresses the ratio between the strain components in the steady-state stage according to (2.2) equals the ratio between the creep-strain-rate components:

$$\varepsilon / \gamma = \sigma / 3.57\,\tau \tag{2.5}$$

and this quantity remained constant in all three stages down to fracture. This latter circumstance indicates that the initial anisotropy originating in the material because of technological treatment does not change during creep until the complete disappearance of the total efficiency of the material.

Table 2 presents values of the dissipation intensity $W_2 = \sigma_{ij}\eta_{ij}^*$ in the steady-state stage of creep, calculated from experimental results, and graphs of the work $A = A$ (t) dissipated during creep are constructed in Fig. 4, where the numbers on the diagram correspond to the numbers of the experiments in Table 2. This material is quite viscous, and the strains reached high values and were computed by means of the dependences

$$\varepsilon = \ln (l / l_0), \quad \gamma = \psi r / (l_0 \exp \varepsilon)$$

where l_0 is the initial sample length, ψ is the angle of twist of the tube, and r is the mean radius. Moreover, the area of the sample cross section was converted for every 2% strain from the condition of incompressibility of the material, and the axial loading and torque were diminished in order to maintain constant values of σ and τ. The experiment was curtailed when strains on the order of 20% were reached. On the whole, all the diagrams proceed in a sufficiently compact bundle practically to fracture. (In the pure-torsion and almost-pure-torsion experiments, a torsional buckling of the tubular sample was observed until the disappearance of the efficiency of the material.) From Table 2 and the graphs of Fig. 4 it is easy to establish that for any level of the dissipated specific work, the ratio of the appropriate times t_2/t_1 remains constant in all stages of creep and agrees with the magnitude of the reciprocal ratio of the mean specific dissipation intensities $W^{(1)}/W^{(2)}$. Therefore, the conclusion that the time of viscous fracture during creep is inversely proportional to the values of the specific dissipation intensities in the steady-state stage, which has been verified for uniaxial loading [2], is valid also for the case of the plane stress state and once more confirms the hypothesis that the specific work dissipated during creep is one of the governing parameters of the viscous fracture of a material, including even anisotropic material.

The results obtained confirm the incontrovertibility of the hypothesis on the existence of creep-strain-rate potential functions and its acceptability to describe processes in anisotropic media.

LITERATURE CITED

1. O. V. Sosnin, "On the anisotropic creep of materials," Zh. Prikl. Mekh. i Tekh. Fiz., No. 6 (1965).
2. A. F. Nikitenko and O. V. Sosnin, "On creep fracture," Zh. Prikl. Mekh. i Tekh. Fiz., No. 3 (1967).